IEEE Access
Multidisciplinary | Rapid Review | Open Access Journal

Received September 2, 2020, accepted September 10, 2020, date of publication September 14, 2020,
date of current version September 25, 2020.

Digital Object Identifier 10.1109/ACCESS.2020.3024031

Improving Accuracy of an Amplitude Comparison-Based Direction-Finding System by Neural Network Optimization

ENQI YAN, XIYE GUO, JUN YANG, ZHIJUN MENG, KAI LIU, XIAOYU LI, AND GUOKAI CHEN
College of Intelligence Science and Technology, National University of Defense Technology, Changsha 410073, China
Corresponding author: Jun Yang (nudtpaper@163.com)

ABSTRACT In the positioning and navigation field, it is essential to use the direction-finding system to obtain the signal direction of arrival (DOA) and target position. The amplitude comparison-based monopulse (ACM) DOA algorithm performs a few calculations, has a simple system structure, and is widely used. The traditional ACM DOA algorithm uses the first-order Taylor expansion to introduce the nonlinear errors, and the angle measurement range is limited. In response to this problem, this study establishes a neural network model for error compensation, and it optimizes the traditional algorithm to obtain a better angle estimation performance. In order to perform an experiment with the proposed algorithm, a novel experimental device was designed. Two measurements at different angles were obtained by rotating the antenna. The ACM angle estimation used only one directional antenna. The results verified the optimization algorithm. The experimental results demonstrated that in comparison with the traditional first-order and the improved third-order Taylor expansion ACM DOA algorithm, the mean absolute error of this method reduced by 81.62% and 72.62%, respectively.

INDEX TERMS Positioning, direction-finding, amplitude comparison, neural network, signal direction of arrival estimation.

I. INTRODUCTION

Presently, satellite navigation and positioning systems are widely used. But in locations such as mines, tunnels, and high-rise ''urban canyons'' in valleys, satellite signals are blocked; hence, they cannot receive and provide accurate positioning services. The pseudo-satellite regional positioning system's appearance offers the possibility to solve the positioning problem in the above scenarios. A pseudolite is a device that is placed on the ground and can emit signals that are similar to the global navigation satellite system (GNSS). The pseudo-satellite station that is established on the ground can enhance the regional satellite navigation and positioning system and also improve the satellite positioning system's reliability and anti-interference ability [1].

With the advent of the 5G era, the large-scale deployment of mobile communication base stations has led to the integration of pseudo-satellite positioning systems and mobile communication systems. The development of integrated navigation and communication systems has broad development prospects. In terms of achieving precise positioning, in addition to traditional mobile cellular positioning technology and GNSS-based satellite navigation and positioning technology, direction-finding positioning methods can also be introduced. On the one hand, the positioning function can be completed independently through direction-finding, and it can also be combined with ranging and positioning to improve the positioning performance.

In terms of the research of direction-finding technology, a multi-channel direction-finding algorithm based on the array antenna and the corresponding system is currently being studied. It has successively proposed the minimum variance distortionless response (MVDR) beamformer algorithm [2], the multiple signal classification (MUSIC) algorithm [3], and the estimation signal parameter via rotational invariance techniques (ESPRIT) method [4]. In particular, the MUSIC algorithm, which is based on the spatial spectrum direction-finding estimation, can provide a high resolution. The MUSIC algorithm needs to search the power spectrum function's peak value to determine the estimated DOA; thus, it requires a considerable amount of calculations. Some scholars have studied and optimized the MUSIC

The associate editor coordinating the review of this manuscript and approving it for publication was Mohammad Tariqul Islam.

algorithm and achieved individual results [5]–[8]. However, for an array antenna-based direction-finding system, each array unit corresponds to the corresponding receiver. Therefore, the implementation of this algorithm requires multiple receiving channels that can be sampled simultaneously, which may introduce additional phases in the actual implementation process, which is difficult to guarantee. The consistency of these multiple receiving channels is ideal [9]–[11]. It is necessary to maintain and calibrate the antenna array, which contains multiple antenna units, and it often brings disadvantages such as complex systems, a large power consumption, and a high cost.

The amplitude comparison-based monopulse (ACM) angle estimation system has a simple structure and it is convenient for installing and deploying a mobile carrier. Many scholars have studied the ACM DOA algorithm and its systems. Reference [12] uses a second-order Taylor expansion approximation to solve the quadratic function extremum and they derived the monopulse angle measurement formula. The authors also presented a theoretical accuracy analysis of the monopulse angle measurement and pointed out the relationship between the monopulse angle measurement error, the beamwidth, and the array signal-to-noise ratio (SNR). The narrower the beamwidth, the higher the SNR and the smaller the angle measurement error. In another study [13], the hardware comparator is not used in the monopulse antenna system, and the sum and difference signal are obtained by performing signal processing to achieve the ACM angle estimation. Priyanka *et al.* [14] proposed a classifier-based amplitude comparison direction-finding (ACDF) algorithm, which uses a fuzzy c-means algorithm and interpolation techniques to enhance the DOA's performance accuracy. In [15], a passive angle estimation using the monopulse correlation method is proposed. Guo and Li [16] further improved the algorithm and solved the direction-finding problem in two steps. The improved algorithm first roughly measures the direction of arrival (DOA), then it only measures the DOA within a limited angular interval, and then it searches for the maximum correlation coefficient; thus, speeding up the algorithm.

However, the traditional ACM DOA algorithm has a practical angle measurement interval. This shortcoming is caused by the algorithm theory itself. In the process of the algorithm, the first-order Taylor expansion formula is used to approximate the received signal. According to the nature of Taylor expansion, a polynomial can be used to approximate the function value at a specific point., The higher the polynomial order, the more accurate the approximation, and the closer to a specific point, the smaller the approximation error. For the traditional ACM algorithm, it provides an angle estimation result with an accuracy higher than the Rayleigh criterion in a smaller angle range near the bisector of the two boresights, but when the signal direction deviates from the bisector, the angle estimation deviation is larger. Iqbal *et al.* [17] proposed a method to reduce the error of the amplitude comparison-based direction-finding system. For signals with a direction of arrival that deviates more from the bisector, they adaptively used adjacent or spare antennas to make the signal as close as possible to the bisector of the two boresights for the DOA measurement. Chengzen C. performed a third-order Taylor series expansion on the adaptive monopulse ratio at the beam center [18]. They applied the polynomial root-finding formula to estimate the target angle, and verified that the method can be improved in comparison with the traditional first-order Taylor series expansion. But in its essence, it applies the Taylor series expansion; thus, the algorithm optimization effect is limited. Therefore, it is of considerable significance to study the ACM DOA algorithm's performance and to improve it.

For complex regression and fitting problems, there are some methods and models that have been proven effective. Multiple regression model and artificial neural network model were established to predict influenza activity, which can accurately reflect influenza epidemic characteristics [19]. Ruan *et al.* [20] compared BP neural network model with linear regression model and Support Vector Machine (SVM) in predicting the citation counts of individual papers. In [21], classification and regression trees model was used to predict blood pressure for people.

In terms of the realization of the direction finding system, some novel ideas have emerged. A two-antenna, single radio-frequency (RF) front-end DOA estimation system is proposed and it extends the measurements to different locations by shifting the antenna tuple together as a single entity [22]. Reference [23] uses two commercial wifi panel antennas to build a convenient system, and uses the amplitude monopulse function to achieve DOA estimation.

In this investigation, we studied the ACM DOA algorithm. For the problem of nonlinear errors in the estimation process, we established a neural network model to compensate for the initial estimation results. This improves the accuracy of the angle estimation results, it enhances the limitation of the original algorithm on the measurement range, and it improves the robustness of the algorithm. We designed a novel test method that uses a single directional antenna to form two antenna beams with a specific angle by rotation. The ACM algorithm is implemented and the effectiveness of the algorithm that is proposed in this study is verified.

The contributions of this investigation are as follows:

1) This study is focused on the shortcomings of the traditional ACM DOA algorithm's active angle measurement interval. In addition, this investigation addresses the limitation of the angle measurement range; thus, a method based on a neural network model is proposed for compensation. Because the first-order Tayler series is used in the bisector of the two boresights, the algorithm has a large error at the position deviating from the bisector. In this study, the neural network model is used to compensate for the error, and then the final DOA estimation result is obtained, which increases the angle measurement performance.

2) This study constructed a novel system that uses only one antenna and one radio frequency (RF) front end. Smart test methods were applied to achieve the traditional ACM DOA algorithm. These methods were tested and they verified the proposed optimization method.

The remainder of this paper is structured as follows. In Section II, the signal model is established, the ACM DOA algorithm is introduced, and the nonlinear error that is introduced by the algorithm is analyzed. In Section III, by focusing on the mistakes in the second part of the analysis, a neural network model is established, and the model is used to compensate for the initial estimation results to obtain the final estimation results. In Section IV, by performing simulation experiments, the proposed method's effectiveness is verified, and the simulation shows the optimization performance of the proposed algorithm under the conditions of the different real signal arrival directions. In Section V, by using a standard gain horn antenna and other related devices, a measurement system was built. In addition, the angle measurement experiments were carried out by using the method that is proposed in this study, which proves the effectiveness of the proposed algorithm. Finally, the conclusion is presented in Section VI.

II. SIGNAL MODEL

The ACM direction-finding system uses multiple directional antennas that are located at the same phase center but with a squint angle difference and it simultaneously receives signals. By comparing the amplitude information of the received signals for the different antennas, the signal arrival direction is estimated. This section takes two antennas as an example to build a signal model and it analyzes the messages that are received by the different antennas.

In order to understand this approach, let us first consider Friis's transmission equation at the receiving antenna for the omni-directional transmission antennas.

$$P_{m,rx} = P_{tx} + G_{tx} + G_{m,rx} + L_c + L_s \tag{1}$$

where m = 1, 2, P_{tx} is the transmitted power, G_{tx} is the transmitter antenna gain, $G_{m,rx}$ is the mth receiver antenna gain, L_c is the cable loss, and L_s is the free space propagation loss. L_s can be calculated as follows.

$$L_s = 20\lg(\frac{c}{4\pi f d_{tx,m}}) \tag{2}$$

where c is the speed of light, f is the carrier frequency, and $d_{tx,m}$ is the distance between the transmitter and the mth receiver.

According to the equation, the difference between the two received signal strengths is determined from Eq. (3).

$$P_{1,rx} - P_{2,rx} = G_{1,rx} - G_{2,rx} \tag{3}$$

According to the above formula, the difference in the received signal strength depends only on the difference in the gain that is between the two receiving antennas. It has nothing to do with the other factors. This is because the different antennas receive signals at different angles and they use the antennas' directional characteristics to obtain the different received signal strengths.

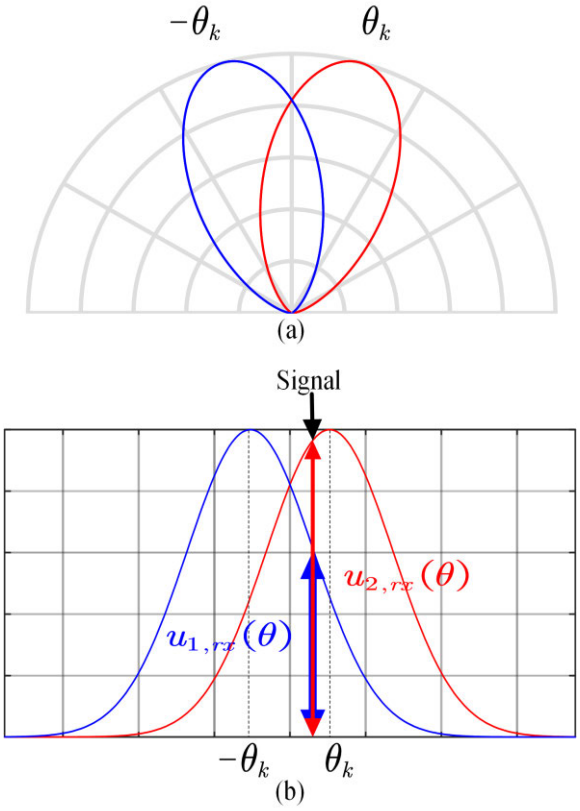

FIGURE 1. Schematic diagram of the ACM angle estimation algorithm. The angle between the two directional antenna is $2\theta_k$. The authentic signal DOA is θ, and the signals received by the two antennas are $u_{1,rx}(\theta)$ and $u_{2,rx}(\theta)$ since the gain difference of the antenna is in different directions.

As shown in the Fig.1, the two beams in the plane partially overlap each other, and the direction of the bisector of the two boresights is known. The antenna squint angle θ_k is also known. Suppose the angle between the direction of the target transmitted signal and the bisector of the two boresights is θ, then the antenna gain pattern function is $g(\theta)$. In this study, the beam pattern is assumed to be a Gaussian pattern [24].

$$g(\theta) = \exp\left[-2\ln 2\left(\theta/\theta_{1/2}\right)^2\right] \tag{4}$$

where $\theta_{1/2}$ is the half-power beamwidth (HPBW) of the beam. According to the received signal strength of the two antennas, it is only determined by the directional antenna gain, which can be expressed as follows.

$$\begin{cases} u_{1,rx}(\theta) = Kg(\theta_k + \theta) \\ u_{2,rx}(\theta) = Kg(\theta_k - \theta) \end{cases} \tag{5}$$

Among them, K is the proportionality factor, which is related to the parameters of the transmitting antenna, the target distance, the target characteristics, and other factors.

According to the ACM DOA algorithm, by using the received signal strength, the sum signal $u_{\sum,rx}(\theta)$ and the

difference signal $u_{\Delta,rx}(\theta)$ can be calculated from $u_{1,rx}(\theta)$ and $u_{2,rx}(\theta)$ as follows.

$$\begin{cases} u_{\sum,rx}(\theta) = u_{1,rx}(\theta) + u_{2,rx}(\theta) = K[g(\theta_k + \theta) + g(\theta_k - \theta)] \\ u_{\Delta,rx}(\theta) = u_{1,rx}(\theta) - u_{2,rx}(\theta) = K[g(\theta_k + \theta) - g(\theta_k - \theta)] \end{cases} \tag{6}$$

Among them, $g_{\sum}(\theta) = g(\theta_k + \theta) + g(\theta_k - \theta)$ is the sum beam pattern, and $g_{\Delta}(\theta) = g(\theta_k + \theta) + g(\theta_k - \theta)$ is the difference beam pattern.

According to the Taylor expansion, when θ tends to be 0 (infinitely close to the bisector of the two boresights), the approximate results can be expressed as follows.

$$\begin{cases} g(\theta_k + \theta) = g(\theta_k) + g'(\theta_k)\theta + o(\theta^2) \approx g(\theta_k) + g'(\theta_k)\theta \\ g(\theta_k - \theta) = g(\theta_k) - g'(\theta_k)\theta + o(\theta^2) \approx g(\theta_k) - g'(\theta_k)\theta \end{cases} \tag{7}$$

The first-order Taylor expansion formula is used to approximate the second order polynomials and above to zero. This processing brings errors to the final angle estimation results, which is also the research content of this paper. In this approximation, the ratio of the sum amplitude of the signal and the signal's difference amplitude the can be expressed as the following Eq. (8).

$$\frac{u_{\Delta,rx}(\theta)}{u_{\sum,rx}(\theta)} = \frac{g'(\theta_k)}{g\theta_k)}\theta = \rho\theta \tag{8}$$

Among them, $\rho = \frac{g'(\theta_k)}{g\theta_k)}$ is the normalized slope coefficient of the antenna pattern at the beam squint angle θ_k.

Through the above derivation, the target signal DOA estimation result can be calculated by applying Eq. (9).

$$\hat{\theta} = \frac{u_{\Delta,rx}(\theta)}{u_{\sum,rx}(\theta)}\frac{1}{\rho} \tag{9}$$

According to the above ACM DOA algorithm and the system model, the block diagram of the algorithm for the angle estimation can be expressed as Fig. 2.

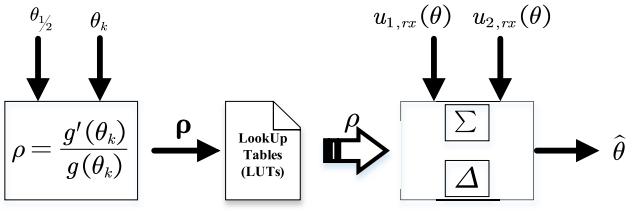

FIGURE 2. Block diagram of the traditional ACM angle estimation algorithm. Before measuring, determine the antenna HPBW $\theta_{1/2}$ and the antenna squint angle θ_k, measure the strength of the received signals of the two antennas, and then calculate the angle estimate $\hat{\theta}$.

Before estimating the target angle, according to the receiving antenna gain pattern function $g(\theta)$, the normalized slope coefficient ρ corresponds to the different θ_k that is calculated and stored in the lookup tables. When it is time to estimate the position of the target signal, look up the normalized slope coefficient ρ that corresponds to $\theta_{1/2}$ and θ_k from the lookup tables, and use the two receiving antennas to obtain the signals $u_{1,rx}(\theta)$ and $u_{2,rx}(\theta)$. Finally, use the above conditions to obtain the DOA estimation result $\hat{\theta}$.

According to the previous introduction and analysis, the traditional ACM DOA algorithm uses a first-order Taylor expansion to approximate the calculation when calculating the normalized slope coefficient, ρ, which introduces errors. Especially for the direction that deviates from the bisector of the two boresights, this method can estimate the angle, the error is substantial, and it is determined by the nature of the Taylor expansion itself. Therefore, the traditional ACM angle estimation algorithm has an effective angle measurement interval in a practical application. In the interval around the bisector of the two boresights, an accurate angle estimation can be obtained. But as the target angle deviates from the bisector of the two boresights, the algorithm is no longer active. Figure 3 uses a Gaussian antenna with an HPBW of 20° as an example to show the theoretical angle estimation performance of the ACM DOA algorithm under the different antenna squint angles without considering the influence of the noise. Fig. 3(a) is a three-dimensional surface diagram which shows the angle estimation error under conditions of different antenna squint angles (θ_k) and different authentic signal DOA. Fig. 3(b) shows four specific conditions of different θ_k.

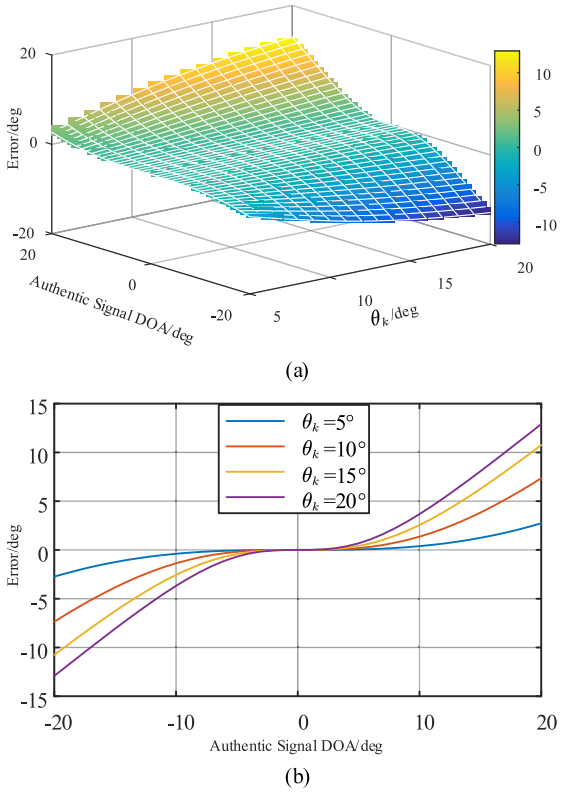

FIGURE 3. The theoretical error of the traditional ACM angle estimation algorithm. The antenna pattern type is Gaussian and the HPBW is 20°. (a) The angle estimation error corresponding to the different antenna squint angles and the different real signal arrival directions. (b) The situations of the squint angles at 5°, 10°, 15°, and 20°.

It can be observed from Fig. 3 that for the traditional ACM DOA algorithm, the angle measurement error, in theory, is smaller in the interval around the bisector of the two boresights. When the real signal arrival direction deviates from the bisector, the algorithm angle measurement error gradually increases. When the true signal arrival direction is 20°, the angle estimation error reaches 13°, which cannot provide a valid angle estimation result. In summary, the traditional ACM algorithm's active angle measurement interval is only near the bisector of the two boresights, which is inconvenient in practical applications. Therefore, to obtain a better target angle estimation performance and to effectively extend the target angle's accurate measurement range, the traditional ACM algorithm needs to be optimized.

III. PROPOSED OPTIMIZATION MODELS

The traditional ACM DOA algorithm performs a first-order Taylor series expansion at the bisector of the two boresights. The angle estimation error at the direction deviating from the bisector has nonlinearity and it is difficult to eliminate through a theoretical calculation. The neural network can fit any nonlinear object with a high accuracy, it has robust nonlinear mapping, and it is easy to implement. It is an effective method to optimize the traditional ACM algorithm by using the neural network method.

A. BASIC MODEL OF THE NEURAL NETWORK

In general, the typical three-layer neural network structure is illustrated in Fig. 4.

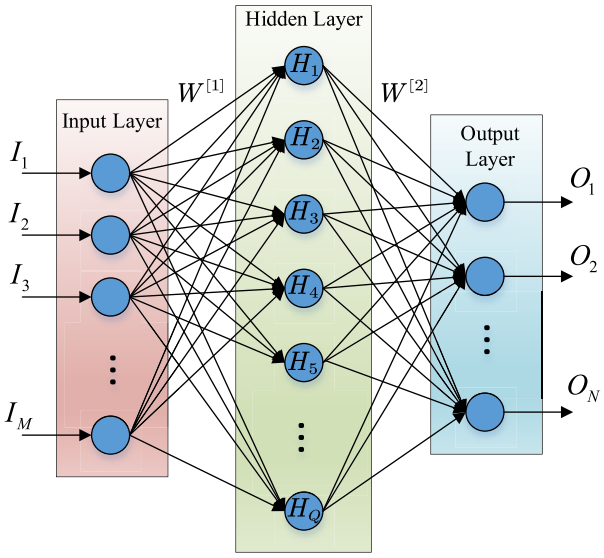

FIGURE 4. Schematic diagram of the three-layer neural network. This includes an input layer, a hidden layer, and an output layer.

In the Fig. 4, $I = [I_1, I_2, I_3, \ldots I_M]^T$ represents the input vector, $O = [O_1, O_2, O_3, \ldots O_N]^T$ represents the output vector of the output layer, and $H = [H_1, H_2, H_3, \ldots H_Q]^T$ represents the output vector of the hidden layer. From the input layer to the hidden layer, a matrix is used to describe the calculation process.

$$H = f_1(W^{[1]}I + b^{[1]}) \tag{10}$$

where $W^{[1]} = [w_{qm}]_{Q\times M}$, which is the weight matrix from the input layer to the hidden layer, $b^{[1]} \in \mathbb{R}^{Q\times 1}$ is the hidden layer's bias matrix, and $f_1(*)$ is the activation function of the hidden layer. Similarly, the calculation expression from the hidden layer to the output layer can be obtained.

$$O = f_2(W^{[2]}H + b^{[2]}) \tag{11}$$

where $W^{[2]} = [w_{nq}]_{N\times Q}$ is the weight matrix from the hidden layer to the output layer, $b^{[2]} \in \mathbb{R}^{N\times 1}$ is the bias matrix of the output layer, and $f_2(*)$ is the activation function of the output layer.

B. THE NEURAL NETWORK-OPTIMIZED AMPLITUDE COMPARISON-BASED MONOPULSE (NN-ACM) ALGORITHM

1) INPUT AND OUTPUT OF THE MODEL

Using the neural network model, the traditional ACM DOA algorithm is optimized, mainly for the case of the deviation from the bisector of the two boresights. This is based on known parameters and accurate DOA estimation results are obtained. According to the analysis of the traditional ACM DOA algorithm in Section II, the parameters that determine the performance of the DOA estimation are mainly the half-power beamwidth and the antenna squint angle. The setting required for the DOA estimation that uses the traditional ACM DOA algorithm is the signal strength that is obtained from two directional antennas. Besides, the noise will also affect the angle estimation result. Therefore, the model is designed as a four-input and one-output model, that is, M = 4 and N = 1. The input variables are the half-power beamwidth (HPBW) $\theta_{1/2}$, the angle $2\theta_k$ between the antenna boresight, the angle calculation result $\tilde{\theta}$ of the traditional ACM DOA algorithm, and the SNR. The output variable is the angle estimation result of the target signal.

2) GENERATION OF THE DATA SET

The influence of the number of training samples on the neural network is reflected in the network's generalization ability. In the ideal case, its training parameters are expected to map the arbitrary functions within the ideal accuracy. According to the structure of the designed neural network model, the selected training samples should cover the situations as much as possible. The value range of each parameter determines the value of each input parameter of the model in the data set. The HPBW $\theta_{1/2}$ values ranging of $[10°, 60°]$ with a step of 10°. Under this condition, the angle of the two antenna boresights $2\theta_k$ takes on the value $[10°, 2\theta_{1/2}]$ with a step of 10°, which ensures that the main lobes of the two antenna beams overlap. The other input parameter in the model is the traditional ACM DOA algorithm's angle calculation result $\tilde{\theta}$. This parameter cannot be given directly, but it is obtained by performing a calculation based on the

received signal. Therefore, when generating the training data set, $\tilde{\theta}$ is calculated by providing the authentic signal DOA θ, and then $\tilde{\theta}$ is used as the input variable of the training set. That is, the range of $\tilde{\theta}$ is determined by θ. Regardless of the changes in the other parameters, any given will always have a corresponding $\tilde{\theta}$. Considering that the algorithm requires the target signal's authentic angle of arrival between the two beams. The value range of θ is $[-\theta_{1/2}, \theta_{1/2}]$ and it has a step of 0.2°. The model also considers the impact of the different noise conditions and it uses the SNR to quantify the noise, its value range is $[-20dB, 20dB]$, and the step is $10dB$. In summary, the variables of the data set are show in Table 1.

TABLE 1. Variables of the data set.

	Variable	Range	Step
Input	$\theta_{1/2}$ /deg	[10, 60]	10°
	$2\theta_k$ /deg	$[10, 2\theta_{1/2}]$	10°
	SNR/dB	[−20, 20]	10dB
	$\tilde{\theta}$ /deg	/	/
Output	θ /deg	$[-\theta_{1/2}, \theta_{1/2}]$	0.2°
Total number of samples		50960	

3) MODEL NORMALIZATION

In order to solve the influence of the dimension between the different data and to improve the accuracy of the neural network model, the input variables and output variables of the model are normalized; hence, the input variables and output variables of the model have the same order of magnitude. When using the model, the output of the model needs to be denormalized. The normalization formula is as follows.

$$y = (y_{\max} - y_{\min})^*(x - x_{\min})/(x_{\max} - x_{\min}) + y_{\min} \quad (12)$$

Among them, $[y_{\min}, y_{\max}]$ is the range of values for the variables after normalization, which is [−1,1] in this study, $[x_{\min}, x_{\max}]$ is the real range of the values for the variables before normalization, and x is the variable being normalized.

4) MODEL TRAINING PARAMETERS

The neural network model's training parameter settings mainly include the number of hidden layer neurons, the maximum number of iterations, the training target, the learning rate, and the activation function. The simplest model uses a three-layer neural network structure, which includes an input layer, a hidden layer, and an output layer. The input and output variables determine the number of neurons in the input layer and the output layer. According to Kolmogorov's theorem [25], M = 4, N = 1, and the neuron of the hidden layer has a value of nine. The maximum number of iterations, $N_{iteration}$, and the training target are used for stopping the training. After reaching either of these two parameters, the training will end and it needs to be set according to the performance of the model. If the learning rate is too small, the model's convergence rate may be too slow, and if the learning rate is too large, the model may not converge. The function of the activation function is to add nonlinear factors to the neural network so that it can solve more complex problems more effectively. The most commonly used activation functions are the Sigmoid function and the rectified linear unit (ReLU) function.

After the above analysis and optimization, the neural network-optimized ACM DOA algorithm can be obtained. The Fig. 5 presents the flow chart of the neural network optimized ACM angle estimation algorithm.

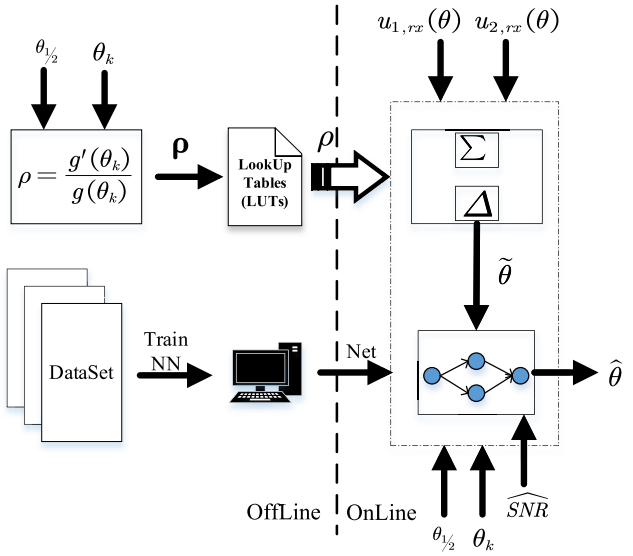

FIGURE 5. The block diagram of the neural network optimized ACM angle estimation algorithm.

Based on the traditional ACM DOA algorithm, the training data set is used to train the neural network, and the training result is saved. According to the diagram, when making an angle estimate, the measurement result is first used to calculate $\tilde{\theta}$ according to the traditional ACM DOA algorithm. Then, the result is inputted into the neural network together with the other conditions ($\theta_{1/2}$, θ_k, $\widehat{SNR}$) to obtain the estimated value $\hat{\theta}$ of the target angle. Among them, $\widehat{SNR}$ can be obtained by the SNR estimation method, which is not the focus of this article and this will not be explained in detail. For the entire process, the neural network training process consumes a lot of computing resources and time; however, it can be performed offline. In actual use, the training results are directly used; thus, it will not significantly impact real-time processing.

IV. ALGORITHM EVALUATION

This section assesses the performance of the proposed neural network-optimized amplitude comparison-based monopulse (NN-ACM) DOA algorithm.

A. ALGORITHM PERFORMANCE OF THE TEST DATA SET

Using the data set in Section III, we randomly selected 60% as the training set, 20% as the verification set, and 20% as

the test set. Through experimentation, the network training parameters with the best performance are determined based on the Table 2.

TABLE 2. Neural network training parameters.

Model parameters	Value
Number of Neurons	9
Maximum Number of Iterations	500
Training Goal	0.0004
Learning Rate	0.1
Activation Function	ReLU

By using the above model parameters, the training data set is used to train the neural network model, and the obtained network model is used to verify the test set. As a comparison, we also used the traditional ACM DOA algorithm and the ACM DOA algorithm that is based on a third-order Taylor expansion to obtain the angle estimation results of the different algorithms.

To quantify and evaluate the performance of the different algorithms, we used the mean absolute error (MAE), mean square error (MSE) and root mean square error (RMSE) to obtain statistics on the three algorithms' results to verify the angle measurement accuracy of the NN-ACM algorithm.

The formulas for MAE, MSE, and RMSE are as follows.

$$MAE = \frac{1}{N}\sum_{n=1}^{N}\left|\hat{\theta}_n - \theta_n\right| \tag{13}$$

$$MSE = \frac{1}{N}\sum_{n=1}^{N}(\hat{\theta}_n - \theta_n)^2 \tag{14}$$

$$RMSE = \sqrt{\frac{1}{N}\sum_{n=1}^{N}(\hat{\theta}_n - \theta_n)^2} \tag{15}$$

In the formula, θ_n is the true angle of the nth sample, $\hat{\theta}_n$ is the estimated angle of the nth sample, and N is the number of samples.

It can be observed from Table 3 that for the test data set, the DOA estimation obtained by the NN-ACM algorithm proposed in this paper, in comparison with the traditional ACM algorithm and the third-order Taylor expansion ACM, the MAE reduced by 82.8% and 77.69%, and the RMSE reduced by 86.5% and 84.5%, respectively.

TABLE 3. Performance metrics of different algorithms.

	MAE	MSE	RMSE
Traditional ACM	5.2320	77.0190	8.7760
Third-Order ACM	4.0351	59.0269	7.6829
NN-ACM	0.9001	1.4003	1.1833

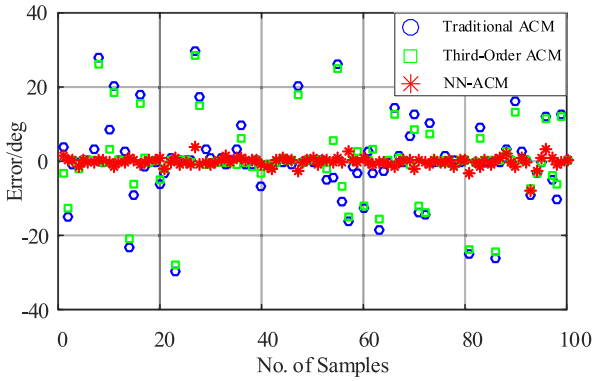

FIGURE 6. Simulation error results of the different algorithms. The blue "O" represents the traditional ACM algorithm, the green "□" represents the third-order Taylor expanded ACM algorithm, and the red "*" represents the NN-ACM algorithm.

In order to accurately show the angle estimation results of the different algorithms, 100 samples were randomly selected from the test data set. This compares the traditional ACM DOA algorithm, the third-order ACM, and the proposed NN-ACM DOA algorithm.

It should be noted that the data of the test set is randomly selected so that each sample may correspond to a different HPBW, different antenna squint angles θ_k, different authentic signal directions of arrival θ, and different SNR conditions, which can represent the performance of the algorithm under a variety of measurement conditions. It can be clearly seen that the proposed NN-ACM DOA algorithm can significantly reduce the angle estimation error.

B. ALGORITHM OVERALL PERFORMANCE VALIDATION

In order to show the performance of the algorithm completely and comprehensively, we used the Monte Carlo method to simulate the angle estimation results of the three algorithms under different conditions. The SNR was set to 20 dB, the HPBW was set to 10°, 20°, 30°, 40°, 50°, 60°, the antenna squint angle θ_k was set so that it equals the HPBW, and the authentic signal arrival direction was set to $[-\theta_k, \theta_k]$. The number of Monte Carlo experiments for each set of parameter conditions was set to 1,000. The specific simulation conditions are presented in Table 4.

According to the simulation results, which are obtained from antennas with different HPBW, the accuracy the DOA estimation results varies with the authentic DOA of the signal, as shown by Fig. 7.

It can be observed from Fig. 7 that for the traditional ACM DOA algorithm, when the real signal arrival direction is near the bisector of the two boresights, the algorithm can accurately estimate the DOA. However, since the actual signal arrival direction deviates from the bisector of the two boresights, the algorithm estimation result gradually becomes more substantial, and the third-order ACM algorithm has a similar rule, which is consistent with the theoretical analysis. For our proposed NN-ACM algorithm, when the real

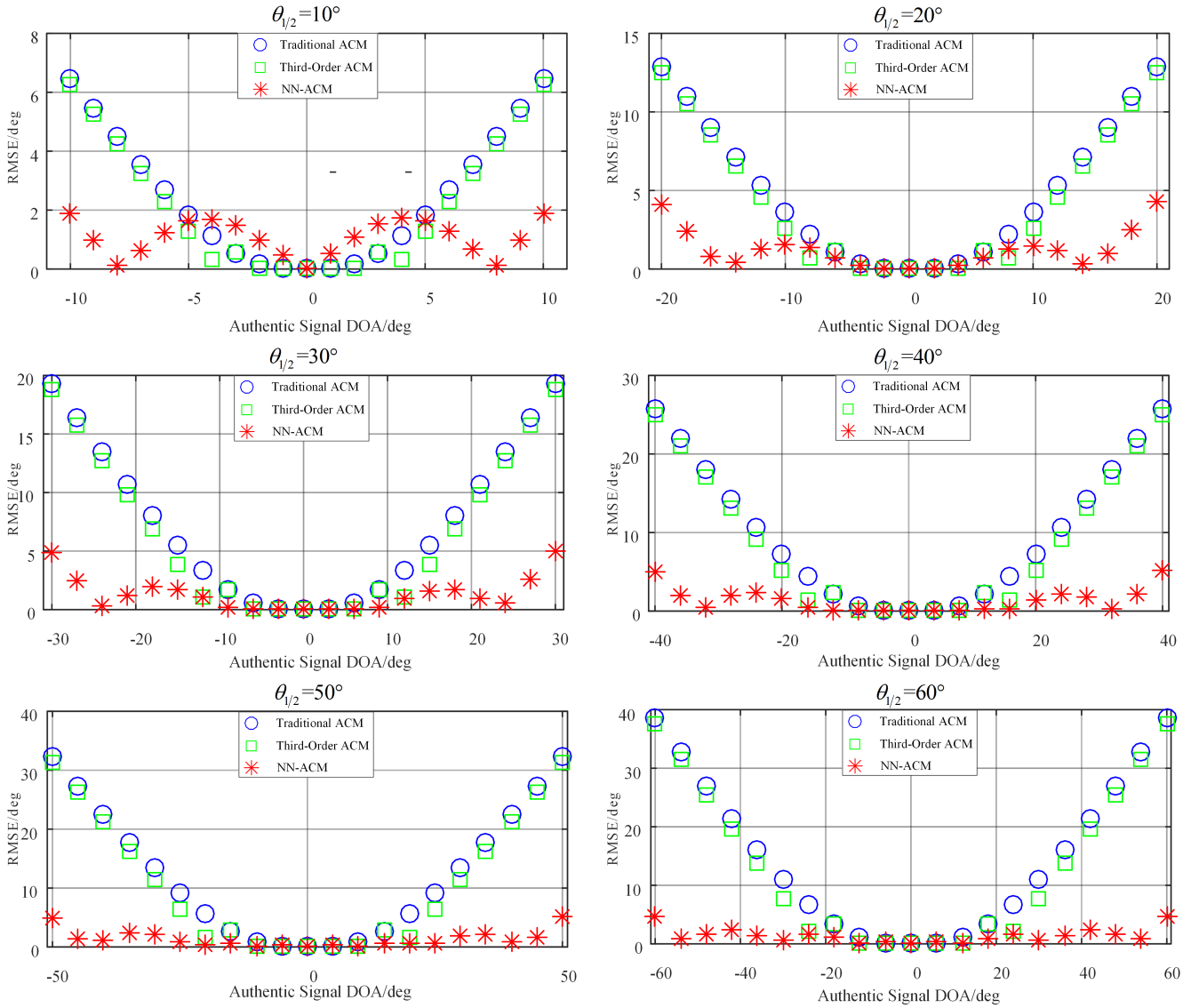

FIGURE 7. Comparison of the Monte Carlo experimental results of the performance of the different algorithms. The HPBW = 10°, 20°, 30°, 40°, 50°, and 60°, the antenna squint angle is equal to the HPBW, the angle estimation mean square root error results correspond to the different real signal arrival directions, and the Monte Carlo times are set to 1000. The blue "○" represents the traditional ACM algorithm, the green "□" represents the third-order Taylor expanded ACM algorithm, and the red "*" represents the NN-ACM algorithm that is proposed in this study.

signal arrival direction is near the bisector of the two boresights, the angle estimation result is close to the traditional ACM algorithm. When the real signal arrival direction deviates from the bisector of the two boresights, the proposed NN-ACM algorithm can avoid large angle estimation errors. For the antenna with the HPBW of 10°, the antenna squint angle of 10°, and the signal arrival direction of 10°, the RMSE of the proposed NN-ACM algorithm is reduced by 70.86% and 69.89% in comparison with the traditional ACM and the third-order Taylor expansion ACM, respectively. For the antenna with the HPBW of 60°, the antenna squint angle of 60°, and the signal arrival direction of 60°, the RMSE indicators of the proposed NN-ACM algorithm are reduced by 88.16% and 87.76% in comparison with the traditional ACM algorithm and the third-order Taylor expansion ACM algorithm, respectively.

The above results show that the proposed NN-ACM algorithm has a better performance for the signal DOA estimation, especially for target signals that deviate significantly from the bisector of the two boresights. This improves the angle measurement accuracy and extends the effective angle measurement range.

V. EXPERIMENT

This section describes a system that uses the traditional ACM algorithm, the third-order Taylor expansion ACM algorithm, and the proposed NN-ACM algorithm to estimate the DOA of the signal and to compare the performance of the algorithms.

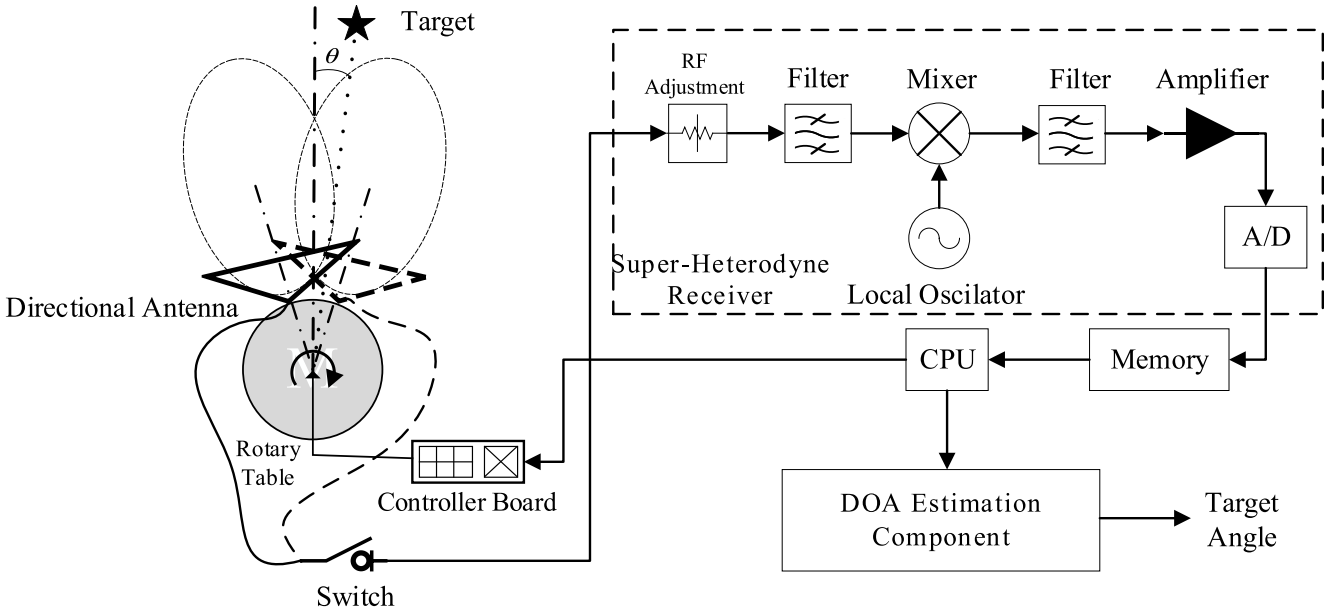

FIGURE 8. The experimental system includes a directional antenna, a rotary table, a receiver, and a DOA estimation component.

TABLE 4. Simulation conditions settings. The dataset can be get according to the simulation settings.

SNR	$\theta_{1/2}$ / deg	θ_k / deg	θ / deg
20 dB	10	10	-10, -9, -8, … 8, 9, 10
	20	20	-20, -18, -16, … 16, 18, 20
	30	30	-30, -27, -24, … 24, 27, 30
	40	40	-40, -36, -32, … 32, 36, 40
	50	50	-50, -45, -40, … 40, 45, 50
	60	60	-60, -54, -48, … 48, 54, 60

A. MEASUREMENT SETUP SYSTEM

The proposed system consists of a directional antenna that is mounted on a rotary table, a controller board, a super-heterodyne receiver with a complex signal recording capability, and the DOA estimation component, as depicted in Fig. 8. The system components prior to the DOA estimation block provide data acquisition. The steps of this process are as follows. First, the antenna is roughly pointed in the target direction, which is recorded as position 1, and it uses the receiver to receive the target signal while measuring the amplitude of the received signal at this time. Second, the rotary table is turned to rotate the antenna by a specific angle $2\theta_k$, and this is recorded as position 2. Third, the receiver obtains the target signal again, and it measures the amplitude of the received signal at this time. This process completes a set of measurements.

In two measurements, the angle of the antenna rotation is accurately controlled by the controller, and its value is passed to the DOA estimation block. In the signal receiving stage, a super-heterodyne receiver is used to process and collect the signals that are received by the antenna. The primary mechanism is to down-convert the high-frequency signal that is received by the antenna into a lower-frequency signal through mixing to facilitate subsequent processing. The signal received from the receiving antenna is doped with noise, and there may be other signal interference outside the signal band. As a result, the first step of processing the received signal is to perform a RF signal adjustment. The preliminary processed signal passes through the mixer, and the signals from the local oscillator are multiplied. After filtering out the high-frequency components in the product, the signal frequency drops from the radio frequency to the intermediate frequency. The analog-to-digital converter (ADC) is used to perform analog-to-digital (A/D) conversion on the intermediate frequency signal to obtain discrete digital sampling results; thus, completing a data acquisition operation. The collected signals are then transmitted to the DOA estimation

block through the central processing unit (CPU). In the DOA estimation module, the acquired digital signal is first calculated by using the correlation method to calculate the amplitude of the measured signal, and then the angle estimation result is obtained. The set-up of the experimental system is presented in Fig. 9.

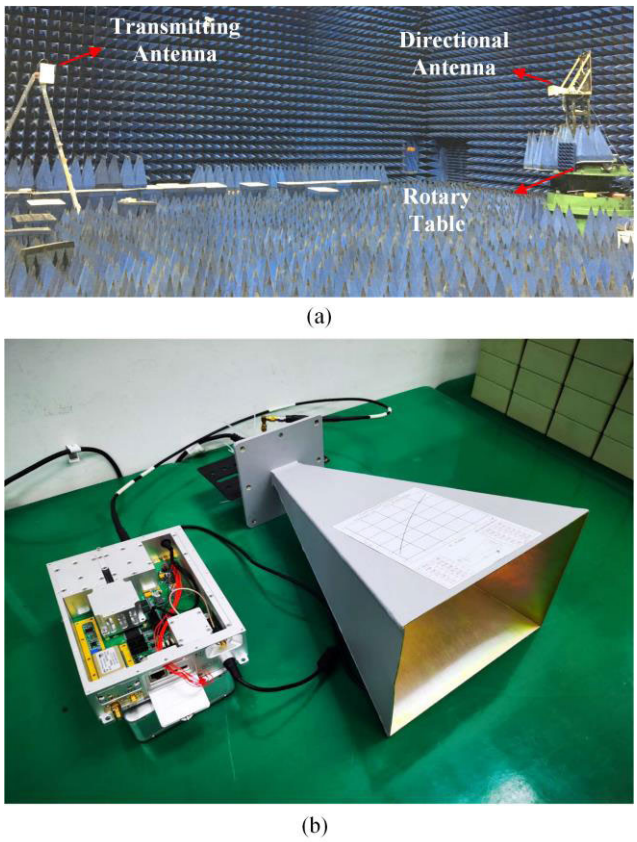

FIGURE 9. Experimental test system. (a) The overall test environment and system. (b) The horn antenna and a signal receiver.

Currently, the DOA estimation component is not embedded in the super-heterodyne receiver but it is completed in a portable computer. Therefore, the data collected by the antenna is first processed by the receiver and then it is dumped into the portable computer through the universal serial bus interface. Based on the algorithm flow that is introduced in Sections II and III, it is executed in the portable computer DOA estimation process. The entire measurement process is carried out in a microwave darkroom to reduce the interference that is caused by the electromagnetic wave reflection.

The specific parameter settings of the experimental system are listed in Table 5.

B. DATA COLLECTION

Before data acquisition and measurement, the antenna is calibrated to obtain the antenna gain pattern, and the gain pattern results are fitted to obtain the pattern function. In order to improve the fitting accuracy, we selected [−30,30] as the range for fitting. Fig. 10 shows the test result and the fitting

TABLE 5. Parameter settings of the experimental system.

	Parameter settings
Receiving Antenna	HD-58SGAH20N 245 *175*450 mm
Signal Model	$s(t) = \sin(2\pi f)$
Signal Frequency	5.845 GHz
Sampling Frequency	60.0 MHz
Laptop Computer	Intel® (R) Core™ i5-8265U CPU @ 1.6 GHz

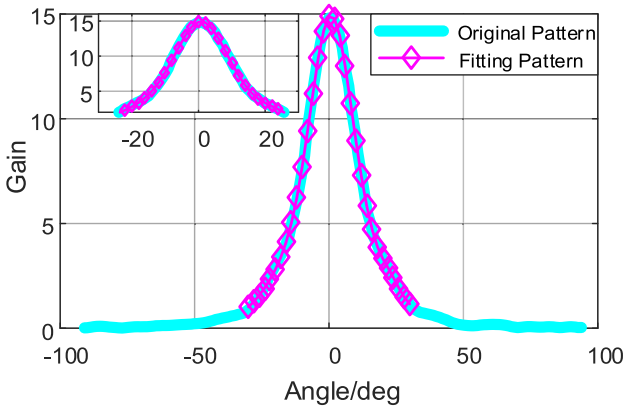

FIGURE 10. The directional antenna HD-58SGAH20N that is used in the experiment. The blue line is the actual test pattern and the red line is the result of fitting the range over [−30°, 30°].

curve of the gain pattern of the horn antenna. According to the calibration results, the antenna has an HPBW of approximately 7°.

To verify the DOA estimation algorithm, the transmitting antenna should transmit signals from different angles of the receiving antenna. It is necessary to measure the direction of the transmitting antenna accurately each time. However, it is not easy to move the transmitting antenna and to accurately measure the direction of the transmitting antenna.

On the other hand, since the receiving antenna is fixed on the turntable, it is accurate and convenient to calibrate the receiving antenna's direction. Using this feature, we have developed a measurement verification scheme that is easy to implement.

① Control the turntable, use the calibration device to align the boresight of the antenna with the transmitting antenna, and record the pointing position of the receiving antenna as $\alpha = 0°$.

② The fixed transmitting antenna does not move; thus, control the turntable and rotate the receiving antenna. Afterwards, make the antenna point from −15° to 15° so it is spaced by 1° for a total of 31 positions. For each position of the transmitting antenna, use the super-heterodyne receiver for the data collection.

③ As described in Section II, using the ACM algorithm to achieve angle estimation requires two signals to be

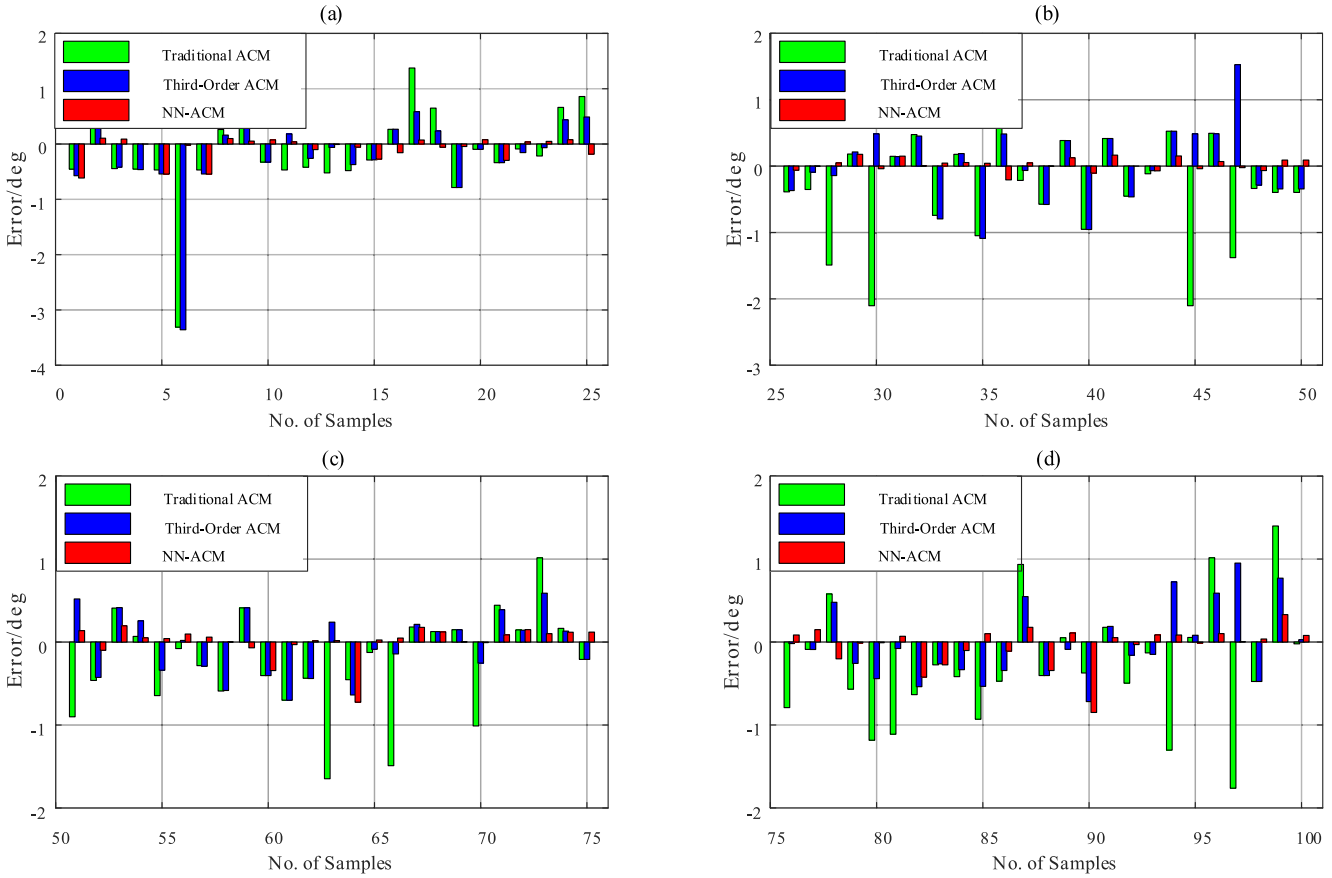

FIGURE 11. Experimental error results of the different algorithms. One hundred sets of the measurement samples were randomly selected. The green histogram represents the traditional ACM algorithm. The blue histogram represents the third-order Taylor expanded ACM algorithm. The red histogram represents the proposed NN-ACM algorithm.

collected. Therefore, the 31 pieces of collected data are divided into two groups: $\alpha_1 \in [-15°, 0°]$ and $\alpha_2 \in [0°, 15°]$. By doing this, $\theta_k = \frac{\alpha_2 - \alpha_1}{2}$ and $\theta = -\frac{\alpha_1 + \alpha_2}{2}$ can be expressed. A total of 256 (16×16) data samples were obtained.

④ To increase the number of samples, repeat step ③ five times, which results in a total of 1280 (256×5) data samples. Take 60% of the data set as the training data set, 20% as the validation data set, and the remaining 20% as the test data set.

C. EXPERIMENTAL RESULTS

Using the measurement results that were obtained in part B, the traditional ACM algorithm, the third-order Taylor expansion ACM algorithm, and the NN-ACM algorithm are used to estimate the angle. Moreover, calculate the MAE indicators of the three algorithms, as listed in Table 6.

It can be observed from Table 6 that in comparison with the traditional ACM algorithm and the third-order Taylor expansion ACM algorithm, the proposed NN-ACM algorithm reduces the MAE indicators by 81.62% and 72.62%, respectively, and the optimization effect is noticeable. By randomly selecting 100 experimental samples from the test data set, the angle estimation error results are shown in the Fig. 11.

TABLE 6. Performance metrics of different algorithms.

Algorithm	MAE	MSE	RMSE
Traditional ACM	0.5935	3.6511	1.9108
Third-Order ACM	0.3985	0.2188	0.4677
NN-ACM	0.1091	0.0237	0.1541

Fig. 11 shows that the third-order ACM algorithm is slightly better than the traditional ACM algorithm, and the proposed NN-ACM algorithm can effectively improve the angle estimation accuracy in comparison with the other two. The angle estimation error is less than 1°.

D. DISCUSSION

In the previous part, we have verified the performance of the proposed NN-ACM algorithm through simulation and experiment, and have compared it with the traditional ACM algorithm and the improved third-order ACM algorithm, which proved that the traditional ACM algorithm can be optimized

by the neural network. Similarly, some other regression models can complete this work. In this part, we use the data set obtained in part B to compare the performance of different regression models, including Line-ar Regression (LR) model, Regression Tree (TR) model, and Support Vector Regression Machine (SVRM). The parameters of different models are shown by Table 7.

TABLE 7. Parameters settings for different models.

	Parameters	Setting value
Linear Regression	/	/
Regression Tree	minimum leaf size	4
SVRM	C	3.7
	gamma	0.35
	kernel	'rbf'

We trained the above three models and compared the performance of them with that of the proposed NN-ACM algorithm. Table 8 shows that some other regression models can also be used to optimize the traditional ACM algorithm to improve the accuracy of angle estimation. The neural network model proposed in this paper has better performance than LR model, RT model, and SVRM. However, it should be noted that the focus of our research is to provide a method that uses neural network to optimize the traditional ACM algorithm to obtain better angle estimation results. In the future, with the development of artificial intelligence and machine learning, there may be models that can achieve better results. This is worth looking forward to.

TABLE 8. Performances of different models.

Models	MAE	MSE	RMSE
LR	0.3743	0.3329	0.5770
RT	0.2182	0.1112	0.3334
SVRM	0.2643	0.0800	0.2828
NN-ACM	0.1091	0.0237	0.1541

VI. CONCLUSION

For the amplitude comparison-based direction-finding systems in the positioning and navigation field, an NN-ACM angle estimation algorithm is proposed in this investigation. This algorithm solves the shortcomings of the traditional algorithm with a smaller angle measurement range. Based on the traditional ACM algorithm, the proposed algorithm uses a neural network model to compensate for the nonlinear error that is caused by the first-order Taylor expansion and it obtains the final angle of the arrival estimation result. The simulation results show that in comparison with the traditional algorithm and the third-order Taylor expansion algorithm, the NN-ACM angle estimation algorithm can improve the angle estimation accuracy. The neural network that is obtained by training is used to verify the algorithm of the test data set. The MAE index of the NN-ACM algorithm proposed in this study reduced by 82.8% and 77.69%, respectively, in comparison with the traditional ACM algorithm and the third-order ACM algorithm.

In this study, we set up a single antenna and a single RF front-end wireless signal DOA estimation system to verify the proposed algorithm. The system uses a standard gain horn antenna. By rotating the antenna to achieve two measurements at different angles, based on the ACM angle estimation algorithm, the signal DOA is estimated. Through experiments, the NN-ACM algorithm that is proposed in this study is verified. In comparison with the traditional ACM angle estimation algorithm and the third-order amplitude comparison-based angle estimation algorithm,the MAE indicators reduce by 81.62% and 72.62%, respectively, the value reaches 0.1091°, and the optimization effect is obvious. Compared with other regression models, the proposed neural network model also performs well.

REFERENCES

[1] N. Kaur and S. K. Sood, "An energy-efficient architecture for the Internet of Things (IoT)," *IEEE Syst. J.*, vol. 11, no. 2, pp. 796–805, Jun. 2017.

[2] J. Capon, "High-resolution frequency-wavenumber spectrum analysis," *Proc. IEEE*, vol. 57, no. 8, pp. 1408–1418, Aug. 1969.

[3] R. Schmidt, "Multiple emitter location and signal parameter estimation," *IEEE Trans. Antennas Propag.*, vol. 34, no. 3, pp. 276–280, Mar. 1986.

[4] R. Roy, A. Paulraj, and T. Kailath, "ESPRIT—A subspace rotation approach to estimation of parameters of cisoids in noise," *IEEE Trans. Acoust., Speech, Signal Process.*, vol. 34, no. 5, pp. 1340–1342, Oct. 1986.

[5] A. Barabell, "Improving the resolution performance of eigenstructure-based direction-finding algorithms," in *Proc. IEEE Int. Conf. Acoust., Speech, Signal Process. (ICASSP)*, Boston, MA, USA, Apr. 1983, pp. 336–339.

[6] D. Wang, R. Chai, and F. Gao, "An improved root-MUSIC algorithm and MSE analysis," in *Proc. Int. Conf. Comput., Inf. Telecommun. Syst. (CITS)*, Kunming, China, Jul. 2016, pp. 1–4.

[7] M. A. Yaqoob, A. Mannesson, B. Bernhardsson, N. R. Butt, and F. Tufvesson, "On the performance of random antenna arrays for direction of arrival estimation," in *Proc. IEEE Int. Conf. Commun. Workshops (ICC)*, Sydney, NSW, Australia, Jun. 2014, pp. 193–199.

[8] A. M. Elbir and T. E. Tuncer, "Compressed sensing for single snapshot direction finding in the presence of mutual coupling," in *Proc. 24th Signal Process. Commun. Appl. Conf. (SIU)*, Zonguldak, Turkey, May 2016, pp. 1109–1112.

[9] K.-L. Du and M. N. S. Swamy, "A deterministic direction finding approach using a single snapshot of array measurement," in *Proc. Can. Conf. Electr. Comput. Eng.*, 2005, pp. 1188–1193.

[10] B. Baygun and Y. Tanik, "Performance analysis of the MUSIC algorithm in direction finding systems," in *Proc. Int. Conf. Acoust., Speech, Signal Process.*, Glasgow, U.K., vol. 4, 1989, pp. 2298–2301.

[11] U. Sarac, F. Harmanci, and T. Akgul, "Experimental analysis of detection and localization of multiple emitters in multipath environments," *IEEE Antennas Propag. Mag.*, vol. 50, no. 5, pp. 61–70, Oct. 2008.

[12] Z. Xu, Y. Huang, Z. Xiong, and S. Xiao, "On the consistency of monopulse and maximal likelihood estimation with array radar," *Modem Radar.*, vol. 35, no. 10, pp. 32–35, Oct. 2013.

[13] T. L. Sheret, C. G. Parini, and B. Allen, "Monopulse sum and difference signals with compensation for a failed feed element," *IET Microw., Antennas Propag.*, vol. 10, no. 6, pp. 645–650, Apr. 2016.

[14] B. Priyanka, V. S. Rani, M. K. Das, and S. Sounak, "An improved amplitude comparison based direction of arrival estimation," *Int. J. Emerg. Technol. Adv. Eng.*, vol. 4, no. 9, pp. 305–311, 2014.

[15] A. A. Loginov and M. Y. Semenova, "Applying correlation method to the problem of passive amplitude monopulse direction finding," in *Proc. IEEE 3rd Int. Conf. Commun. Softw. Netw.*, Xi'an, China, May 2011, pp. 66–68.

[16] D. L. Guo and Z. H. Li, "A fast direction finding algorithm based on correlation processing," *Appl. Mech. Mater.*, vols. 373–375, pp. 880–883, Aug. 2013.
[17] M. F. Iqbal, Z. Khalid, M. Zahid, and A. Abdullah, "Accuracy improvement in amplitude comparison-based passive direction finding systems by adaptive squint selection," *IET Radar, Sonar Navigat.*, vol. 14, no. 5, pp. 662–668, May 2020.
[18] C. Chengzen, "Monopulse angle estimation with adaptive array based on the third-order Taylor series," *Modern Radar*, vol. 35, no. 8, pp. 32–36, Aug. 2013.
[19] H. Xue, Y. Bai, H. Hu, and H. Liang, "Influenza activity surveillance based on multiple regression model and artificial neural network," *IEEE Access*, vol. 6, pp. 563–575, 2018.
[20] X. Ruan, Y. Zhu, J. Li, and Y. Cheng, "Predicting the citation counts of individual papers via a BP neural network," *J. Informetrics*, vol. 14, no. 3, Aug. 2020, Art. no. 101039.
[21] B. Zhang, Z. Wei, J. Ren, Y. Cheng, and Z. Zheng, "An empirical study on predicting blood pressure using classification and regression trees," *IEEE Access*, vol. 6, pp. 21758–21768, 2018.
[22] A. Gorcin and H. Arslan, "A two-antenna single RF front-end DOA estimation system for wireless communications signals," *IEEE Trans. Antennas Propag.*, vol. 62, no. 10, pp. 5321–5333, Oct. 2014.
[23] M. Poveda-Garcia, J. A. Lopez-Pastor, A. Gomez-Alcaraz, L. M. Martinez-Tamargo, M. Perez-Buitrago, A. Martinez-Sala, D. Canete-Rebenaque, and J. L. Gomez-Tornero, "Amplitude-monopulse radar lab using WiFi cards," in *Proc. 48th Eur. Microw. Conf. (EuMC)*, Madrid, Spain, Sep. 2018, pp. 464–467.
[24] Y. J. Han, J. W. Kim, S. R. Park, and S. Noh, "An investigation into the monopulse radar using tx-rx simulator in electronic warfare settings," in *Proc. Symp. Korean Inst. Commun. Inf. Sci.*, Jeongseon, South Korea, Jan. 2017, pp. 705–706.
[25] V. Kůrková, "Kolmogorov's theorem and multilayer neural networks," *Neural Netw.*, vol. 5, no. 3, pp. 501–506, Jan. 1992.

ENQI YAN received the B.S. degree from the College of Intelligence Science and Technology, National University of Defense Technology, in 2018, where he is currently pursuing the M.S. degree. His research interests include signal processing, ground-based positioning, and navigation technology.

XIYE GUO received the B.S., M.S., and Ph.D. degrees from the College of Mechatronics Engineering and Automation, National University of Defense Technology, China, in 2003, 2005, and 2010, respectively. From December 2016 to February 2017, he was a Visiting Scholar with the University of New South Wales (UNSW). He is currently an Associate Research Fellow with the College of Intelligence Science and Technology, National University of Defense Technology. His current research interests include global navigation satellite systems, navigation augmentation, and precise positioning and timing.

JUN YANG received the B.S., M.S., and Ph.D. degrees from the College of Mechatronics Engineering and Automation, National University of Defense Technology, China, in 1994, 1999, and 2007, respectively. He is currently a Professor with the College of Intelligence Science and Technology, National University of Defense Technology. His teaching and research interests include signal processing, space instruments, global navigation satellite system applications, and intelligent satellite.

ZHIJUN MENG received the Ph.D. degree in instrument science and technology from the National University of Defense Technology (NUDT), China, in 2017. He is currently an Assistant Research Fellow with the College of Intelligence Science and Technology, NUDT. His research interests include digital signal processing, on-board intelligent processing platform, inter-satellite link of navigation constellation, and high-precision ranging and time synchronization.

KAI LIU received the M.S. degree in instrument science and technology from the National University of Defense Technology, in 2016, where he is currently pursuing the Ph.D. degree with the College of Intelligence Science and Technology. His research interests include global navigation satellite system positioning, global navigation satellite system signal processing, and pseudolite application.

XIAOYU LI received the B.S. degree from the College of Intelligence Science and Technology, National University of Defense Technology, in 2018, where he is currently pursuing the M.S. degree. His research interests include ground-based positioning and navigation technology.

GUOKAI CHEN received the B.S. degree in measurement and control technology from the National University of Defense Technology, in 2019, where he is currently pursuing the Ph.D. degree with the College of Intelligence Science. His research interests include complex environment positioning and spatial machine intelligence.